This is a repository copy of *Searching for nova shells around cataclysmic variables -- II. A second campaign*.

White Rose Research Online URL for this paper:
https://eprints.whiterose.ac.uk/181693/

Version: Submitted Version

Searching for nova shells around cataclysmic variables - II. A second campaign.

D. I. Sahman,[1]* V. S. Dhillon[1,2].

[1]*Department of Physics and Astronomy, University of Sheffield, Sheffield S3 7RH, UK*
[2]*Instituto de Astrofísica de Canarias, E-38205 La Laguna, Tenerife, Spain*

ABSTRACT

We report on our second campaign to search for old nova shells around cataclysmic variables (CVs). Our aim was to test the theory that nova eruptions cause cycles in the mass transfer rates of CVs. These mass transfer cycles change the behaviour of CVs during their inter-eruption periods. We examined Hα images of 47 objects and found no new shells around any of the targets. Combining our latest results with our previous campaign (Sahman et al. 2015), and the searches by Schmidtobreick et al. (2015) and Pagnotta & Zurek (2016), we estimate that the nova-like phase of the mass transfer cycle lasts ∼3,000 years.

Key words: stars: novae, cataclysmic variables.

1   INTRODUCTION

Cataclysmic variables (CVs) are close binary systems in which a white dwarf (WD) primary accretes material from a late-type secondary star via Roche-lobe overflow (see Warner 1995 for a review). Non-magnetic CVs are classified into 3 main sub-types – the classical novae, the dwarf novae and the nova-likes. The *classical novae* (CNe) are defined as systems in which only a single nova eruption has been observed. Nova eruptions have typical amplitudes of 10 magnitudes and are believed to be due to the thermonuclear runaway of hydrogen-rich material accreted onto the surface of the white dwarf. The *dwarf novae* (DNe) are defined as systems which undergo quasi-regular (on timescales of weeks–months) outbursts of much smaller amplitude (typically 6 magnitudes). Dwarf novae outbursts are believed to be due to instabilities in the accretion disc causing it to collapse onto the white dwarf (Osaki 1974). The *nova-like* variables (NLs) are the non-eruptive CVs, i.e. objects which have never been observed to show novae or dwarf novae outbursts. The absence of dwarf novae outbursts in NLs is believed to be due to their high mass-transfer rates, producing ionised accretion discs in which the disc-instability mechanism that causes DNe outbursts is suppressed; the mass transfer rates in NLs are $\dot{M} \sim 10^{-9}$ M$_\odot$ yr^{-1} whereas DNe have rates of $\dot{M} \sim 10^{-11}$ M$_\odot$ yr^{-1} (Warner 1995).

Mass transfer is believed to be driven by angular momentum loss, which in turn is driven by two main processes,

mass loss from magnetically-coupled winds from the secondary star (commonly referred to as *magnetic braking*), and gravitational wave emission. At periods longer than about 3 hours, both mechanisms operate, leading to high $\dot{M}$ as seen in NLs. At orbital periods below two hours, only gravitational wave emission occurs, and $\dot{M}$ is lower, as in DNe. However, the orbital period distribution of CVs shows both high and low $\dot{M}$ systems co-existing at the same orbital periods (Knigge et al. 2011).

One explanation for the coexistence of systems at the same orbital period with high and low $\dot{M}$ is a nova-induced cycle. Some fraction of the energy released in the nova event will heat up the WD, leading to irradiation and subsequent bloating of the secondary. Following the nova event, the system would have a high $\dot{M}$ and appear as a NL. As the WD cools, $\dot{M}$ reduces and the system changes to a DN, or even possibly $\dot{M}$ ceases altogether and the system goes into hibernation. Hence CVs are expected to cycle between nova, NL and DN states, on timescales of $10^4 - 10^5$ yrs (Shara et al. 1986, Bode & Evans 2008). This nova-induced cycle theory became known as hibernation theory

Hibernation theory was originally invoked to explain the disparity between the observed space density of CVs compared to models. Recent surveys using Gaia DR2 data (Pala et al. 2020) compared to more sophisticated models (Belloni et al. 2018) have shown that the space density of CVs is broadly in agreement with theoretical predictions. However, we still need to understand the impact of the nova eruption on the evolution of CVs. Recent modelling by Hillman et al. (2020) predicts that some systems are expected to

* E-mail: david.sahman@sheffield.ac.uk

cease mass transfer after a nova eruption and go into hibernation, though far fewer systems that exhibit this behaviour are predicted than were first proposed in the original version of the theory (Shara et al. 1986). Recently however, Schaefer (2020) reported measurements the orbital period changes of six of CNe, using a long term monitoring campaign and archival data. He found that five of them showed a period decrease across the nova eruption. This is exactly the opposite of the model predictions, which suggest that the orbital period should increase as the two stars are driven apart during the nova eruption.

The cyclical evolution of CVs through CN, NL and DN phases has received observational support from the discovery that BK Lyn appears to have evolved through all three phases since its likely nova outburst in the year AD 101 (Patterson et al. 2013). A second piece of evidence has come from the discovery of nova shells associated with the dwarf novae Z Cam, AT Cnc and Nova Sco 1437 (Shara et al. 2007, Shara et al. 2012, Shara et al. 2017). However, the association of these CVs with the historical Chinese and Korean records has been reviewed by Hoffmann (2019), who found that all three are doubtful.

A more obvious place than DNe to find nova shells is around NLs, as the nova- induced cycle theory suggests that the high $\dot{M}$ in NLs is due to a recent nova outburst. This was the motivation behind our first campaign to search for nova shells, reported in Sahman et al. (2015, hereafter S15). We discovered a nebula around the nova-like V1315 Aql, which was subsequently confirmed as a nova shell using Keck DEIMOS spectroscopy (Sahman et al. 2018). Other shells have since been discovered around other novalikes. IPHASX J210204.7+471015 is a NL at the centre of a shell originally thought to be a planetary nebula (Guerrero et al. 2018). V341 Ara is another NL at the centre of a shell originally thought to be a planetary nebula (Castro Segura et al. 2021). BZ Cam is located in a bow-shock nebula with faint circular filaments, and is possibly associated with the ancient nova in AD 369 (Hoffmann & Vogt 2020).

Our first campaign, which relied on Hα images obtained with both the Auxiliary Port Camera on the 4.2m William Herschel Telescope (WHT) and the 2.5m Isaac Newton Telescope (INT) Photometric Hα Survey of the Northern Galactic Plane (IPHAS), suffered from two drawbacks. First, the field of view of the WHT was too small to detect the large shells which have been discovered around DNe (Shara et al. 2007, Shara et al. 2012), and also contained too few field stars to derive a reliable stellar point spread function (PSF) which allows one to detect shells close to the CVs. The second problem was that the wide–field IPHAS survey was too shallow, and was targeted at the Galactic plane which has large background Hα nebulosity, making it difficult to detect faint nova shells.

In this paper, we report on our second, much deeper and wider–field campaign to identify old nova shells around CVs, and use our results, combined with other searches, to estimate the lifetime of the nova-like phase following a nova eruption.

2   TARGET SELECTION, OBSERVATIONS, AND DATA REDUCTION

2.1   Target selection

This second campaign was motivated by the shortcomings of our original campaign in S15. We had estimated the age of the faintest shell we could detect with the WHT by simulating images using the old nova DQ Her. The simulations showed that we could expect to detect shells at ~ 180 yr after outburst. This detection threshold can be pushed fainter, and hence older by ~ 40 years, by computing the mean radial profile of the PSF of the central object and inspecting the wings for evidence of a shell, a technique pioneered by Gill & O'Brien (1998).

However, using DQ Her led us to underestimate the optimal field of view for hunting for nova shells. This is because DQ Her has relatively slow-moving ejecta ($350\,\mathrm{km\,s^{-1}}$; Warner 1995). The angular size of a nova shell is determined by the time since the nova eruption, the distance to the CV, and the speed of the ejecta, and is given by the following scaling relation:

$$R \sim 20'' \, \frac{t/100\,\mathrm{yr} \times v/1000\,\mathrm{km\,s^{-1}}}{d/\mathrm{kpc}}, \qquad (1)$$

where R is the angular radius of the shell in arcseconds, t is the time elapsed since the nova eruption, v is the shell expansion velocity, and d is the distance to the CV. Hence a recent, distant nova with slow-moving ejecta ($t = 100\,\mathrm{yr}, v = 500\,\mathrm{km\,s^{-1}}, d = 2\,\mathrm{kpc}$) would have a small shell of radius $\sim 5''$, whereas an older, nearby nova with fast moving ejecta ($t = 200\,\mathrm{yr}, v = 2000\,\mathrm{km\,s^{-1}}, d = 0.5\,\mathrm{kpc}$) would have expanded to a radius of $\sim 2.7'$. The field of view of the Auxiliary Port Camera on the WHT ($\sim 1'$ radius) used for S15, was too small to detect such large shells. This is borne out by the size of the shell that we discovered around V1315 Aql (Sahman et al. 2018), which is $\sim 2.5'$ in radius, the shell around IPHASX J210204.7+471015 which has a radius of $\sim 2.0'$ (Guerrero et al. 2018), and the shells discovered by Shara et al. (2007, 2012) of radii 1.5′ (AT Cnc) and 15′ (Z Cam). A further problem with having such a small field of view is the paucity of field stars that are available to compare radial profiles (see Section 3.1).

Whilst the IPHAS survey had a sufficiently large field of view ($\sim 17'$ radius per pointing) to discover nova shells, it suffered from very short exposure times (120 s). Furthermore, IPHAS was constrained to the Galactic plane, making it difficult to pick out faint nova shells from the bright background Hα nebulosity. We concluded that a more optimal survey for nova shells would have approximately the same field of view as an IPHAS pointing, avoid the Galactic plane and be of similar depth to our WHT survey (~ 25 mags/arcsec^2).

To ensure we only targeted relatively well-studied systems with reliable periods and CV classifications, we made our selection from version 7.20 of the catalogue of Ritter & Kolb (2003)[1] (hereafter RK catalogue). We deliberately selected a substantial number of the systems in the 3–4 hr orbital period range, which is where most NLs appear, as shown in Fig. 18 of Knigge et al. (2011).

---

[1] http://www.mpa-garching.mpg.de/RKcat/

We included a number of asynchronous polars in the target list. Asynchronous polars are CVs with a highly magnetic WD, in which the WD spin period is not synchronous with the orbital period. One possible cause of the asynchronicity is believed to be a nova eruption (Campbell & Schwope 1999). The target list also included a few DNe as a control sample and to ensure that we had sufficient targets visible on each night. All targets were outside the central galactic plane, with a galactic latitude $b > \pm 5^o$.

2.2 Observations

We were allocated three nights on the INT in August 2014 and three nights in January 2015. We were also allocated time from the service observing programme which resulted in an additional 10 targets being observed. We observed 47 targets in total, primarily NLs, including 16 systems that we had previously examined in S15 using the WHT. The targets comprised one old nova (which is also an intermediate polar), three asynchronous polars, 39 NLs, and four DNe.

We used the WFC mounted at the prime focus of the INT. The WFC consists of 4 thinned e2v 2kx4k CCDs and has a platescale of $0.33''$ per pixel, with a field of view of $\sim 34' \times 34'$. In order to cover the gaps in the CCD array, we took sets of four images dithered by $20''$ up and down, and right and left.

We used the Hα filter no. 197, which is centred on Hα and has a FWHM of 95Å. Note that this filter also includes a contribution from N[II] 6584Å emission, which may dominate the spectra of nova shells with strong shock interaction of the ejecta with any pre-existing circumstellar medium, e.g. T Pyx (Shara et al. 1989). We also used the Sloan r band filter no. 214 (centred on 6240Å with FWHM 1347Å).

A full list of the 47 objects and a journal of observations is given in Table1 1. The observing conditions were generally good, with seeing below $2''$. There was some cloud on the nights of 15 December 2014, and 22 February 2015, and on those nights the seeing also worsened to $3''$ and $4''$, respectively.

2.3 Data reduction

The images were processed using the data reduction pipeline THELI (Schirmer 2013). Bias correction was carried out using bias frames taken at the start and the end of the night. Flat-fielding was performed using twilight flats. The astrometry was performed using SCAMP (Bertin 2006), with standard astrometric catalogues (eg. PPMXL, USNO, 2MASS). The processed images were co–added by taking the median. No sky subtraction was performed to avoid the accidental removal of faint nova shells.

3 RESULTS

3.1 INT Images and Radial Profiles

In order to detect shells in the images, we adopted two strategies. First, we visually examined each image to determine if a shell is visible. This technique reveals shells with diameters of more than a few arcseconds. Second, we calculated the radial profile (PSF) of each CV and compared it
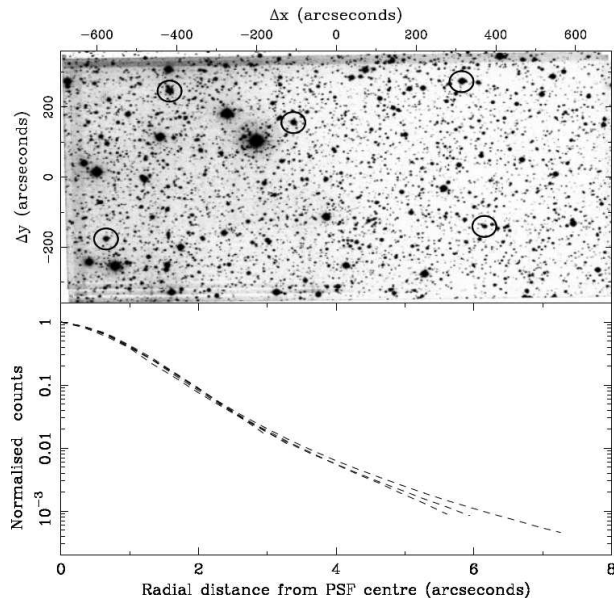

Figure 1. PSF Test for one of the CCDs in the WFC. The PSFs of the circled stars in the upper frame are plotted in the lower frame. Due to nearby stars, the maximum radial distance plotted varies for each star.

to the radial profiles of a number of field stars in the same image. Any nebulosity around the CV due to a nova shell would cause the radial profile of the CV to lie above the average profile of the field stars. This technique can reveal shells with diameters of less than a few arcseconds, and was successfully used by Gill & O'Brien (1998) to discover four new nova shells. We also used this technique in S15. A key assumption in this technique is that the radial profile of the PSF is uniform across the field of view. Fig 1 shows the PSFs for various field stars (circled) in the image of V1432 Aql. The PSFs show identical radial profiles irrespective of field position, giving confidence that the PSFs are uniform across the field of view of the CCD, as expected.

The images and radial profiles of our 47 targets are shown in Appendix A, except for the image of V1315 Aql which is presented in Sahman et al. (2018). Note that the contrast in the images has been optimised. The background sky level appears white and any emission brighter than a few percent above the background, including the stars, appears black. This emphasises any faint nebular emission. As a result, the background levels of each of the four chips appears slightly different in some of the images.

3.2 Notes on Individual Targets

There are some noteworthy features in the images and radial profiles of individual targets that we discuss below:

- BZ Cam has a radial profile above the field stars because of emission from the pre-existing bow-shock nebula. Hoffmann & Vogt (2020) proposed that this system could be a recurrent nova instead of a NL.
- The asynchronous polar V1500 Cyg has a pronounced peak in its radial profile at around $5''$, from the nova event in 1975 (Lindegren & Lindgren 1975).

Table 1. Journal of observations (in alphabetical order of constellation). The classifications and orbital periods of the CVs have been taken from the RK catalogue (Ritter & Kolb 2003). The date refers to the start time of the first exposure.

Object	Classification	Orbital period (hrs)	Date	UTC start	UTC end	Number of exposures	Total exposure time (secs)	Visible shell?
PX And	NL SW NS SH	3.51	01/08/14	04:43	05:16	2	1800	N
			04/08/14	03:18	03:42	4	1080	N
HL Aqr	NL UX SW	3.25	04/08/14	00:27	02:10	8	3840	N
UU Aqr	NL UX SW SH	3.93	01/08/14	03:16	04:36	7	3780	N
V794 Aql	NL VY	3.68	03/08/14	22:39	23:37	6	2880	N
V1315 Aql	NL UX SW	3.35	01/08/14	22:45	01:55	13	8700	Y
V1432 Aql	NL AM AS	3.37	02/08/14	21:43	23:16	32	3840	N
WX Ari	NL UX SW	3.34	15/01/15	20:37	22:01	8	3840	N
KR Aur	NL VY NS	3.91	18/01/15	01:26	02:45	8	3840	N
BY Cam	NL AM AS	3.35	15/01/15	23:48	01:26	8	3840	N
BZ Cam	NL VY SH	3.69	16/12/14	05:19	05:34	1	900	N
			17/01/15	00:20	01:40	8	3840	N
V482 Cam	NL SW	3.21	18/01/15	02:49	04:06	8	3840	N
V425 Cas	NL VY	3.59	04/08/14	02:15	03:14	6	2880	N
			27/10/15	22:43	23:29	3	2700	N
CH Crb	NL UX SW	3.49	23/02/15	06:09	06:24	1	900	N
V1500 Cyg	Na NL AM AS	3.35	01/08/14	02:23	02:57	3	2100	N
V2275 Cyg	Na IP	7.55	02/08/14	03:28	04:07	2	1800	N
			03/08/14	23:43	00:22	4	1920	N
CM Del	NL UX VY	3.89	02/08/14	01:12	02:37	8	3840	N
MN Dra	DN SU ER	2.40	02/08/14	23:20	01:03	8	3840	N
OZ Dra	NL UX SW	3.28	18/01/15	05:16	06:17	6	2880	N
			02/03/15	02:25	03:27	4	3600	N
V1084 Her	NL SW NS	2.89	02/03/15	03:31	04:34	4	3600	N
BH Lyn	NL SW SH NS	3.74	16/01/15	01:11	02:39	8	3840	N
			29/01/15	01:27	01:42	1	900	N
BP Lyn	NL UX SW	3.67	17/01/15	02:20	03:39	8	3840	N
			29/01/15	01:45	02:00	8	3840	N
HQ Mon	NL UX	7.58	16/12/14	04:15	04:30	1	900	N
V380 Oph	NL VY SW NS	3.70	28/05/15	23:58	01:00	4	3600	N
V1193 Ori	NL UX SW NS	3.96	17/01/15	21:32	23:10	8	3840	N
LQ Peg	NL VY SH NS	2.99	02/08/14	02:44	03:22	4	1920	N
FY Per	NL VY	6.20	15/01/15	22:05	23:36	8	3840	N
LX Ser	NL VY SW	3.80	03/08/14	21:12	22:33	8	3840	N
			17/01/15	06:03	06:55	3	2700	N
			18/01/15	06:19	06:24	3	180	N
			02/03/15	04:38	05:40	4	3600	N
RW Sex	NL UX	5.88	17/01/15	03:44	05:05	8	3840	N
			29/01/15	03:18	03:33	8	3840	N
SW Sex	NL UX SW	3.24	16/01/15	04:50	06:10	8	3840	N
V1294 Tau	NL VY SW	3.59	16/01/15	21:26	22:51	8	3840	N
			13/10/15	02:07	02:58	3	2700	N
RW Tri	NL UX SW	5.57	04/08/14	03:46	04:46	6	2880	N
DW UMa	NL SW SH NS	3.28	16/01/15	03:28	04:46	8	3840	N
			29/01/15	03:37	03:52	1	900	N
			23/02/15	04:12	04:59	3	2700	N
LN UMa	NL VY SW	3.47	18/01/15	04:11	05:08	6	2880	N
UX UMa	NL UX	4.72	16/01/15	06:15	06:59	6	2880	N
			17/01/15	05:09	05:57	6	2880	N
			01/03/15	03:15	04:16	6	3600	N
SS UMi	DN SU ER	1.63	01/08/14	21:32	22:35	4	3600	N
			02/08/14	21:16	21:29	1	240	N
HS0220+0603	NL UX SW	3.58	17/01/15	19:55	21:19	8	3840	N
HS0229+8016	NL UX VY	3.88	16/01/15	19:59	21:22	8	3840	N
HS0455+8315	NL VY SW	3.57	18/01/15	00:03	01:23	8	3840	N
HS1813+6122	NL UX SW NS	3.55	13/10/15	21:37	22:24	3	2700	N
			27/10/15	21:14	21:29	1	900	N

Table 1 – *continued*

Object	Classification	Orbital period (hrs)	Date	UTC start	UTC end	Number of exposures	Total exposure time (secs)	Visible shell?
J0506+7725	DN SU	1.62	28/10/15	03:11	04:13	4	3600	N
J0809+3814	NL SW	3.21	29/01/15	01:07	01:22	1	900	N
J0928+5004	NL UX	10.04	29/01/15	02:04	02:19	1	900	N
J1429+4145	NL	1.64	23/02/15	05:03	06:05	4	3600	N
J1924+4459	NL SW SH NS	2.75	27/10/15	21:36	22:38	4	3600	N
Leo5	DN ZC	3.51	28/05/15	22:44	23:46	4	3600	N
LSIV-083	NL UX	4.69	29/05/15	01:11	02:13	4	3600	N
RXJ0524+4244	NL AM AS	2.62	16/01/15	23:17	00:17	8	3840	N
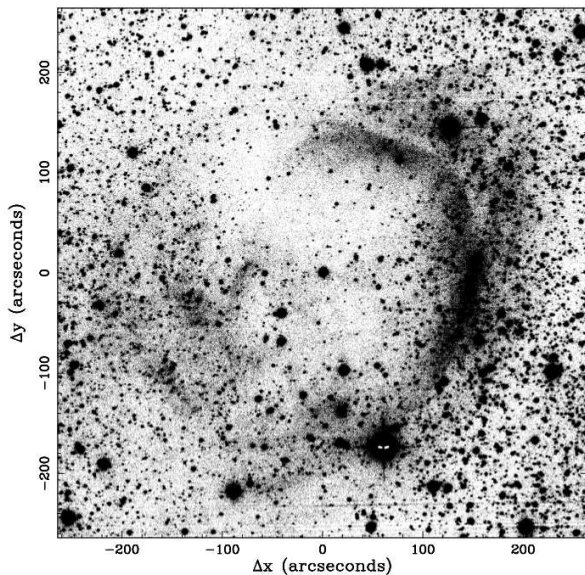
Figure 2. INT WFC Hα image of the nova shell around V1315 Aql. The binary is located at the centre of the image. North is up and East is left.

• V2275 Cyg was discussed extensively in S15, where we discovered a number of Hα blobs in IPHAS images that appeared to move over time. We attributed this apparent motion to a light echo from the 2001 nova eruption. The blobs are not discernible in our image, which was taken six years after the last IPHAS image used in S15.

• CM Del lies in a crowded field, and is blended with a nearby star. Hence its radial profile is artificially enlarged.

• FY Per has a number of nearby stars and hence the radial profile has an unreliable shape.

• J1429+4145 is extremely faint in our image and we were unable to derive a radial profile.

A number of the brighter targets were over–exposed, which leads to the saturation of the central pixels and gives the radial profile a flat–top profile. The targets affected were HL Aqr, UU Aqr, V1084 Her, RW Tri and LSIV-083. Despite being saturated, the wings of the radial profiles are still useful for detecting small shells. None of the other radial profiles of our targets showed any significant deviation

from the field stars, implying that there were no small shells around any of the targets.

3.3 Combined results of our two campaigns and other recent work

In Table 2 we summarise the combined results from S15 and our second campaign reported in this paper, which shows that we have examined a total of 132 CVs, including 51 NLs. Table 2 also shows the results from two other similar campaigns by Schmidtobreick et al. (2015) and Pagnotta & Zurek (2016), neither of whom found shells around the CVs they examined.

4 DISCUSSION

Our new survey brings the total number of NLs that have been observed to 56 (see Table 2), with one nova shell discovered around the nova-like V1315 Aql (Sahman et al. 2018). What can we deduce from this? Given the much increased rate of nova detection in the last century, let us assume that any novae eruptions in these NLs that occurred in the last ∼100 years would have been observed. These would now be classified as old novae in the RK catalogue and hence would not appear in our sample of NLs. We also know from our simulations (see Section 2.1) that our observations are not sensitive to shells older than ∼200 yrs. Hence our search for nova shells around NLs is only likely to find shells between ∼100 and ∼200 years old. We found one shell in this ∼100-year window, out of 56 NLs surveyed, indicating that the lifetime of the NL phase lasts approximately ∼5,600 yrs.

If we include the discovery of the nova shell around IPHASX J210204.7+471015 by Guerrero et al. (2018), who used a similar setup, in our calculation then we have two NLs with shells from a total of 57 NLs. Assuming the ∼100-year visibility window as discussed in the previous paragraph, this would imply a NL lifetime of ∼3,000 yrs. This result is broadly consistent with the order-of-magnitude estimate of 1,000 years derived by Patterson et al. (2013) for the NL phase of CVs.

Schmidtobreick et al. (2015) found no shells around the 15 CVs they examined. They derived a lower limit of 13,000 years for the overall nova recurrence time. This is consistent with the lifetime of the NL phase of ∼3,000 yrs that we have derived, as one would expect that the NL phase should be

Table 2. Summary of our search for nova shells.

	Nova-like Variables	Polars & Intermediate Polars	Asynchronous Polars	Dwarf Novae	Old Novae	Total
Original paper (Sahman et al. 2015)						
WHT Targets	22	1	2	2	4	31
IPHAS Targets	5	10	2	34	23	74
less: Duplicated objects	−3				−1	−4
Total	24	11	4	36	26	101
This Paper	39	1	3	3	1	47
less: Duplicated objects	−12	−1	−3			−16
Total	51	11	4	39	27	132
Schmidtobreick et al. (2015)	5			10		15
Pagnotta & Zurek (2016)		1	3			4
less: Duplicated objects			−3			−3
Grand total	56	12	4	49	27	148

shorter than the overall nova recurrence time, assuming that the cyclical evolution theory is correct.

The latest models by Hillman et al. (2020) show that the behaviour of a CV during a nova cycle is largely determined by the masses of the two component stars. They modelled four CVs, with WDs of mass 0.7 $M_\odot$ and 1.0 $M_\odot$ and secondaries of mass 0.45 $M_\odot$ and 0.7 $M_\odot$. They found that the high mass pair were most likely to exhibit high mass transfer rates, and hence appear as NLs, whereas the low mass pair only achieved NL mass transfer rates just prior to a nova eruption, and only during the phase when both magnetic braking and gravitational wave radiation were operating. This suggests that both V1315 Aql and IPHASX J210204.7+471015 are more likely to harbour high mass components.

The search by Pagnotta & Zurek (2016) for nova shells around three asynchronous polars and one intermediate polar found no shells. Their aim was to test the theory that the asynchronicity of the WD spin was caused by past nova eruptions (Campbell & Schwope 1999). Our search included three asynchronous polars, V1432 Aql, BY Cam, and V1500 Cyg. Two of these, V1432 Aql and BY Cam, were observed by Pagnotta & Zurek (2016). Our observations were not as deep as theirs, and we had a smaller field of view so, unsurprisingly, we also found no shells.

5 CONCLUSIONS

We performed a second Hα-imaging survey to search for old nova shells around CVs. We imaged 47 CVs with the INT and found no new shells. Assuming that the nova-induced cycle theory is correct, our results, when combined with our previous campaign and other recent similar surveys, imply that the nova-like phase for CVs lasts ∼3,000 years.

6 DATA AVAILABILITY

Data available on request.

REFERENCES

Belloni D., Schreiber M. R., Zorotovic M., Iłkiewicz K., Hurley J. R., Giersz M., Lagos F., 2018, MNRAS, 478, 5626

Bertin E., 2006, in Gabriel C., Arviset C., Ponz D., Enrique S., eds, Astronomical Data Analysis Software and Systems XV Vol. 351 of Astronomical Society of the Pacific Conference Series, Automatic Astrometric and Photometric Calibration with SCAMP. p. 112

Bode M. F., Evans A., 2008, Classical Novae. Cambridge University Press

Campbell C. G., Schwope A. D., 1999, A&A, 343, 136

Castro Segura N., Knigge C., Acosta-Pulido J. A., Altamirano D., del Palacio S., Hernandez Santisteban J. V., Pahari M., Rodriguez-Gil P., Belardi C., Buckley D. A. H., Burleigh M. R., Childress M., Fender R. P., Hewitt D. M., James D. J., Kuhn R. B., Kuin N. P. M., Pepper J., Ponomareva A. A., Pretorius M. L., Rodríguez J. E., Stassun K. G., Williams D. R. A., Woudt P. A., 2021, MNRAS, 501, 1951

Gill C. D., O'Brien T. J., 1998, MNRAS, 300, 221

Guerrero M. A., Sabin L., Tovmassian G., Santamaría E., Michel R., Ramos-Larios G., Alarie A., Morisset C., Bermúdez Bustamante L. C., González C. P., Wright N. J., 2018, ApJ, 857, 80

Hillman Y., Shara M., Prialnik D., Kovetz A., 2020, Advances in Space Research, 66, 1072

Hoffmann S. M., 2019, MNRAS, 490, 4194

Hoffmann S. M., Vogt N., 2020, MNRAS, 497, 1419

Knigge C., Baraffe I., Patterson J., 2011, ApJS, 194, 28

Lindegren L., Lindgren H., 1975, Nat, 258, 501

Osaki Y., 1974, Pub. Astr. Soc. Japan, 26, 429

Pagnotta A., Zurek D., 2016, MNRAS, 458, 1833

Pala A. F., Gänsicke B. T., Breedt E., Knigge C., Hermes J. J., Gentile Fusillo N. P., Hollands M. A., Naylor T., Pelisoli I., Schreiber M. R., Toonen S., Aungwerojwit A., Cukanovaite E., Dennihy E., Manser C. J., Pretorius M. L., Scaringi S., Toloza O., 2020, MNRAS, 494, 3799

Patterson J., Uthas H., Kemp J., de Miguel E., Krajci T., Foote J., Hambsch F.-J., Campbell T., Roberts G., Cejudo D., Dvorak S., Vanmunster T., Koff R., Skillman D., Harvey D., Martin B., Rock J., Boyd D., Oksanen A., Morelle E., Ulowetz J., Kroes A., Sabo R., Jensen L., 2013, MNRAS, 434, 1902

Ritter H., Kolb U., 2003, A&A, 404, 301, (Update RKCat 7.20, 2013)

Sahman D. I., Dhillon V. S., Knigge C., Marsh T. R., 2015, MNRAS, 451, 2863

Sahman D. I., Dhillon V. S., Littlefair S. P., Hallinan G., 2018, MNRAS, 477, 4490

Schaefer B. E., 2020, MNRAS, 492, 3343

Schirmer M., 2013, ApJS, 209, 21

Schmidtobreick L., Shara M., Tappert C., Bayo A., Ederoclite A., 2015, MNRAS, 449, 2215

Shara M. M., Ilkiewicz K., Mikolajewska J., Pagnotta A., Bode M. F., Crause L. A., Drozd K., Faherty J. K., Fuentes-Morales I., Grindlay J. E., Moffat A. F. J., Schmidtobreick L., Stephenson F. R., Tappert C., Zurek D., 2017, Nat, 548, 558

Shara M. M., Livio M., Moffat A. F. J., Orio M., 1986, ApJ, 311, 163

Shara M. M., Martin C. D., Seibert M., Rich R. M., Salim S., Reitzel D., Schiminovich D., Deliyannis C. P., Sarrazine A. R., Kulkarni S. R., Ofek E. O., Brosch N., Lépine S., Zurek D., De Marco O., Jacoby G., 2007, Nat, 446, 159

Shara M. M., Mizusawa T., Wehinger P., Zurek D., Martin C. D., Neill J. D., Forster K., Seibert M., 2012, ApJ, 758, 121

Shara M. M., Potter M., Williams R. E., Cohen J., 1989, ApJ, 337, 720

Warner B., 1995, Cataclysmic Variable Stars. Cambridge University Press, Cambridge
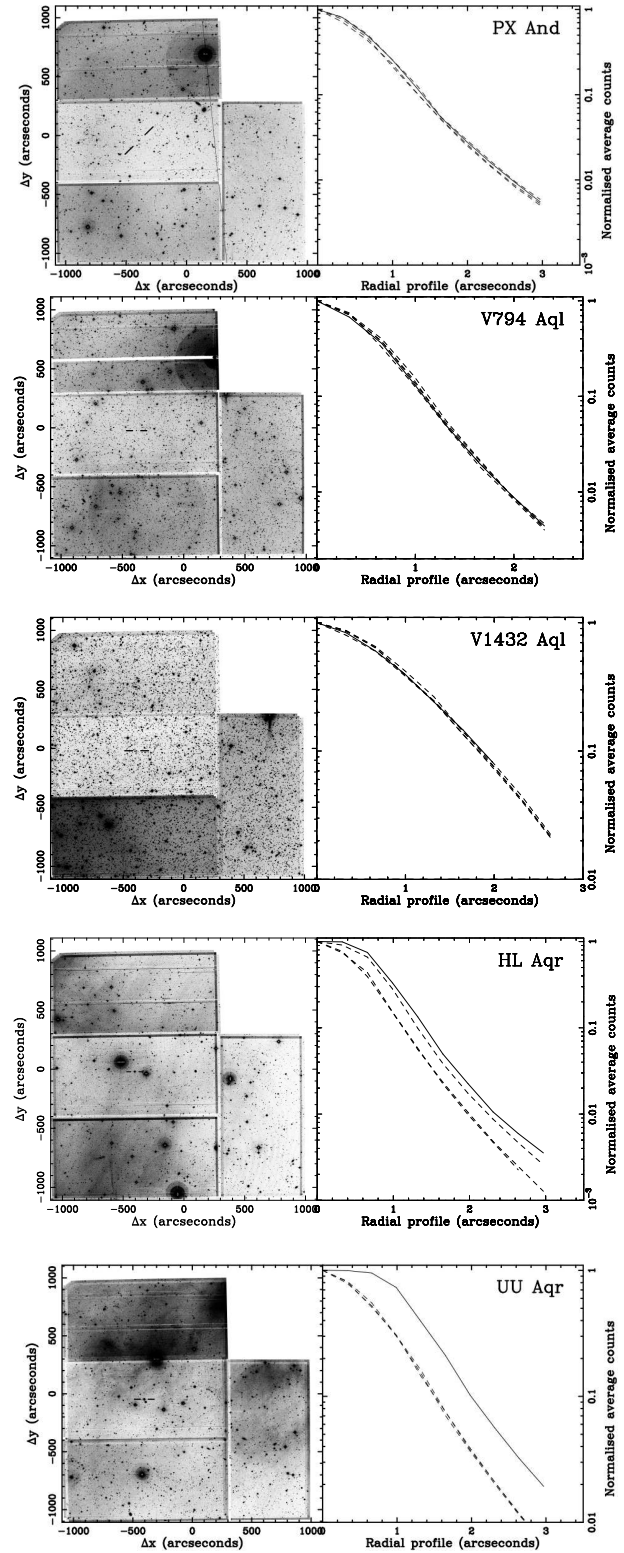
APPENDIX A: INT IMAGES

Figure A1. INT images of our target CVs in order of constellation. The CV lies at the centre of the middle CCD on the left-hand side and is indicated by tick marks. In all images, North is up and East is left. Right: Radial profiles of our targets (solid lines) and field stars (dashed lines).
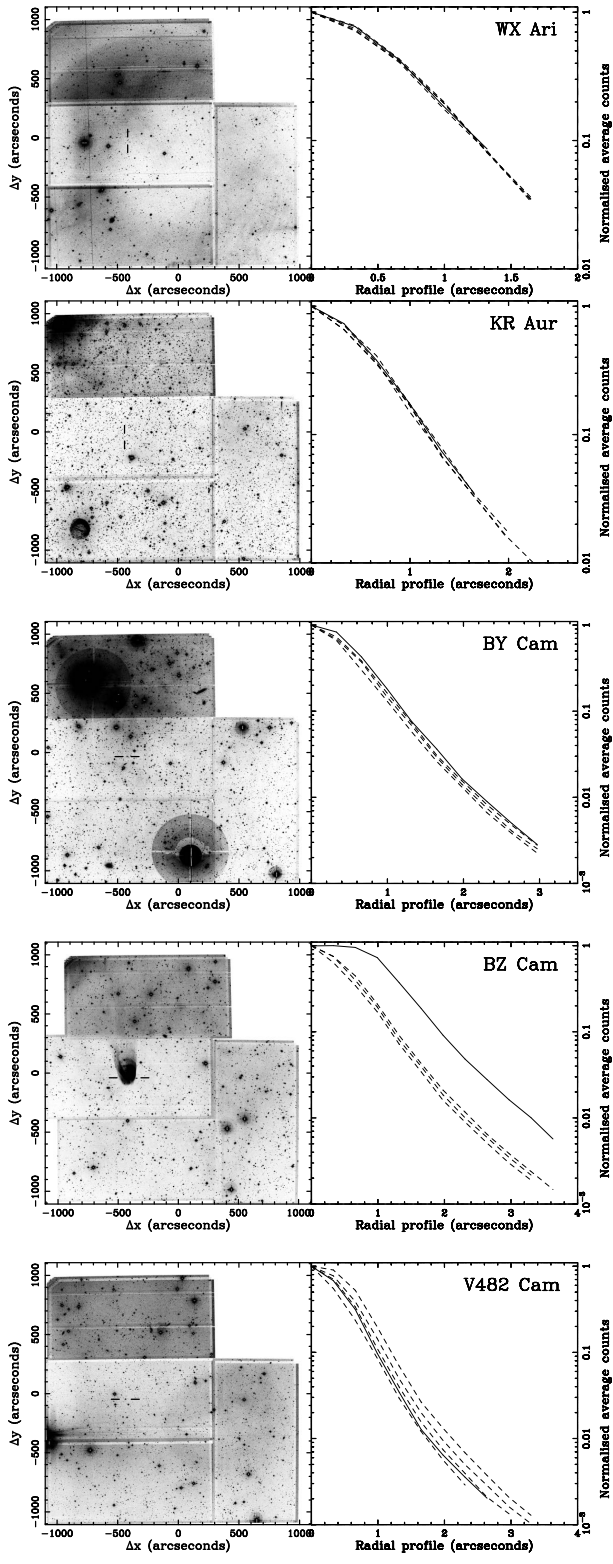
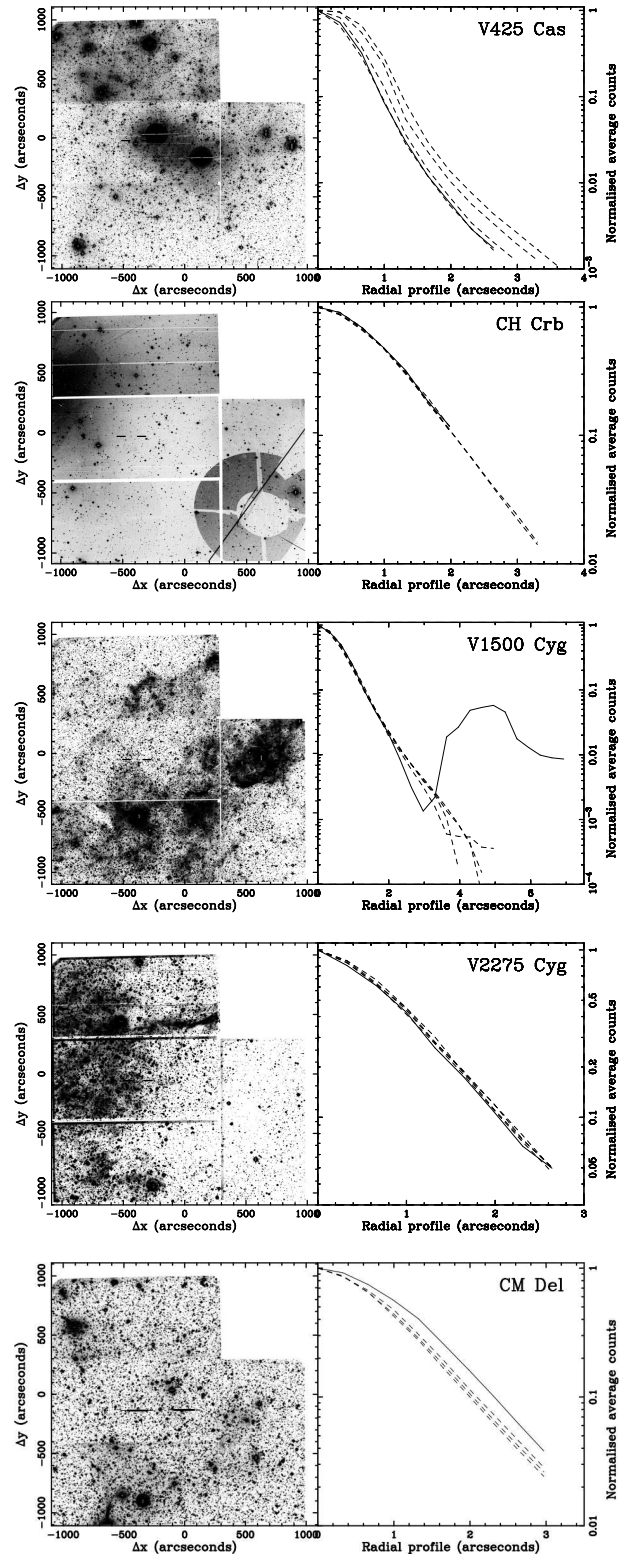**Figure A2.** See caption to Figure A1 for details.

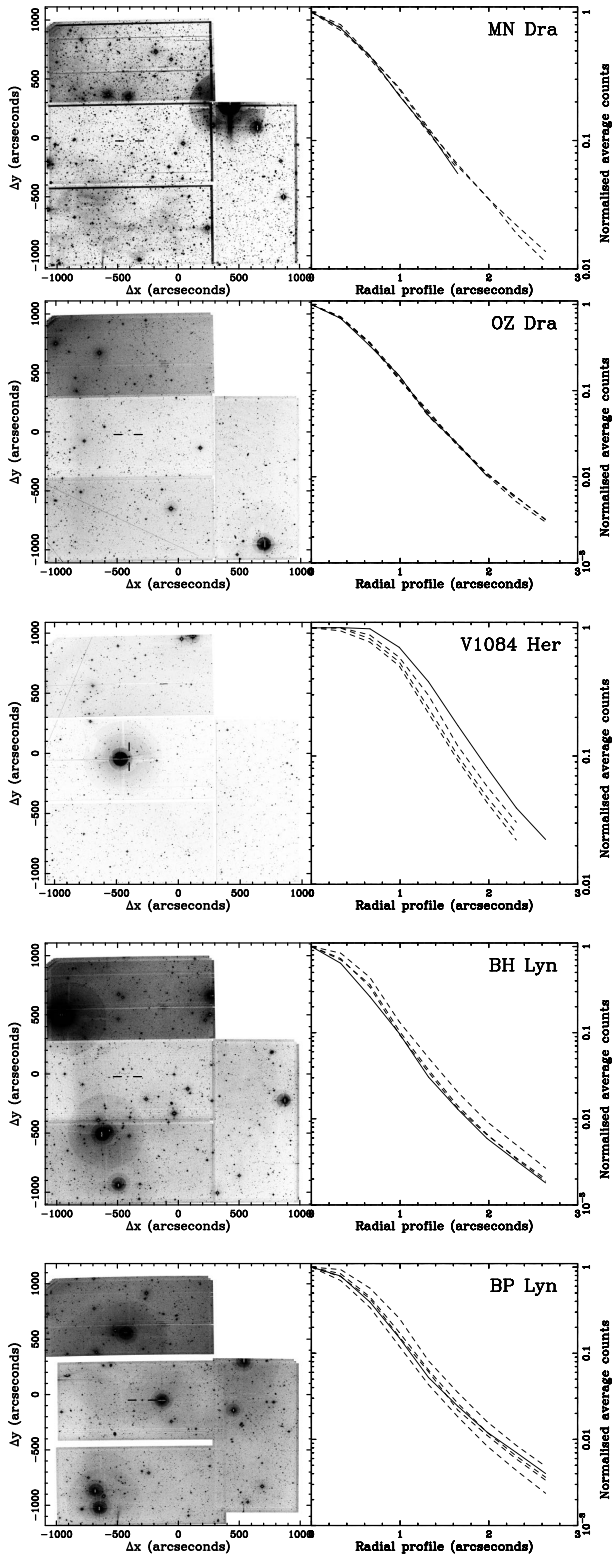**Figure A3.** See caption to Figure A1 for details.
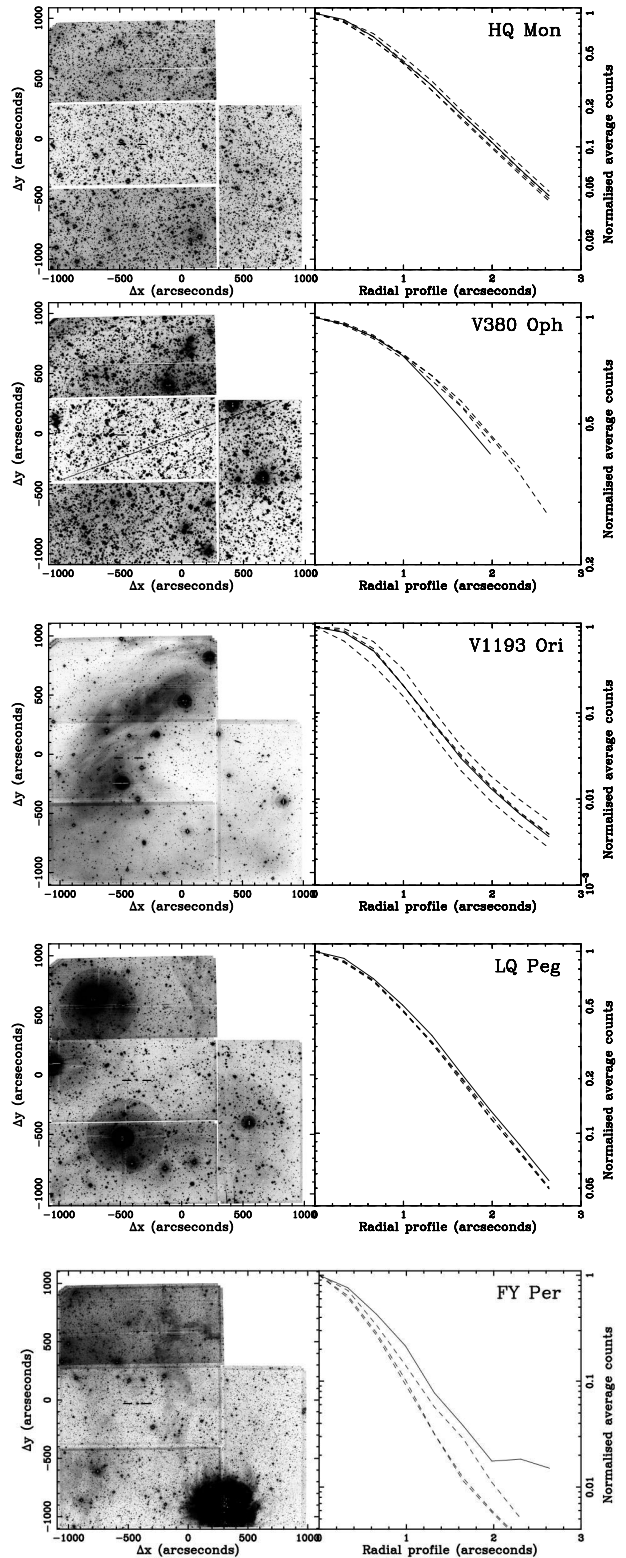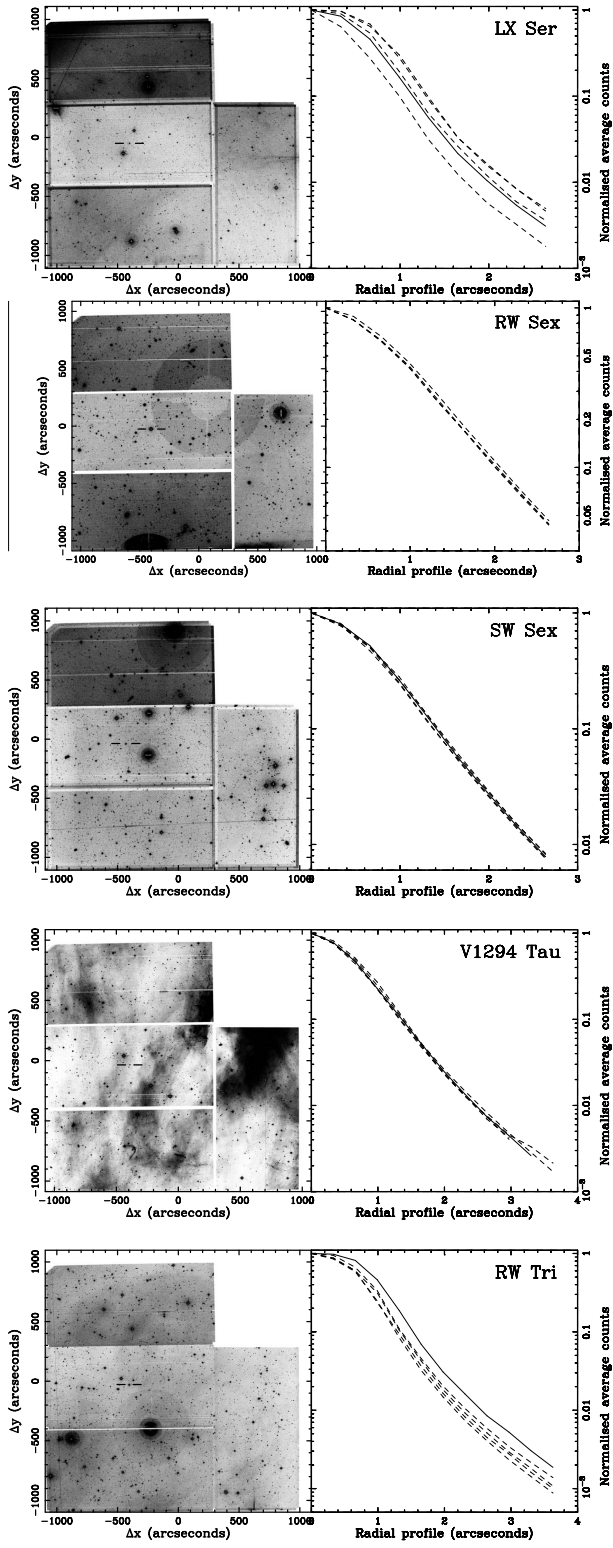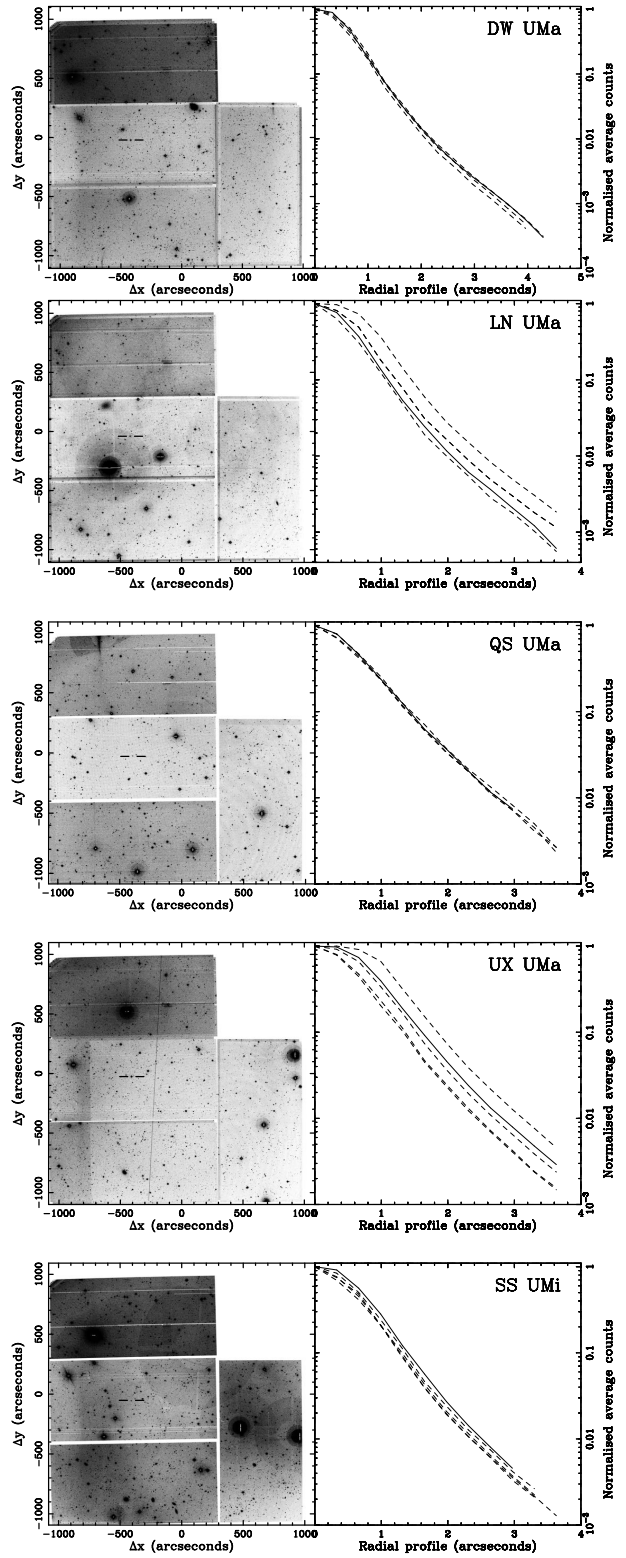
Figure A4. See caption to Figure A1 for details.

Figure A5. See caption to Figure A1 for details.

Figure A6. See caption to Figure A1 for details.
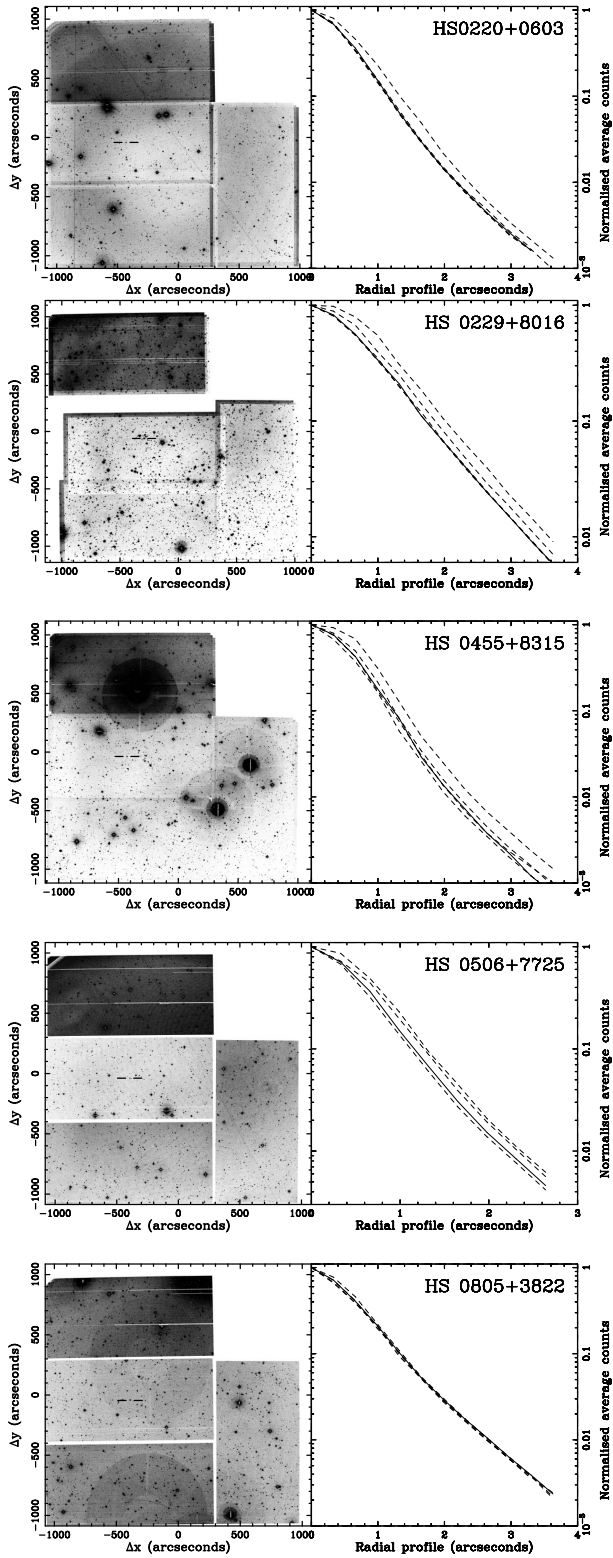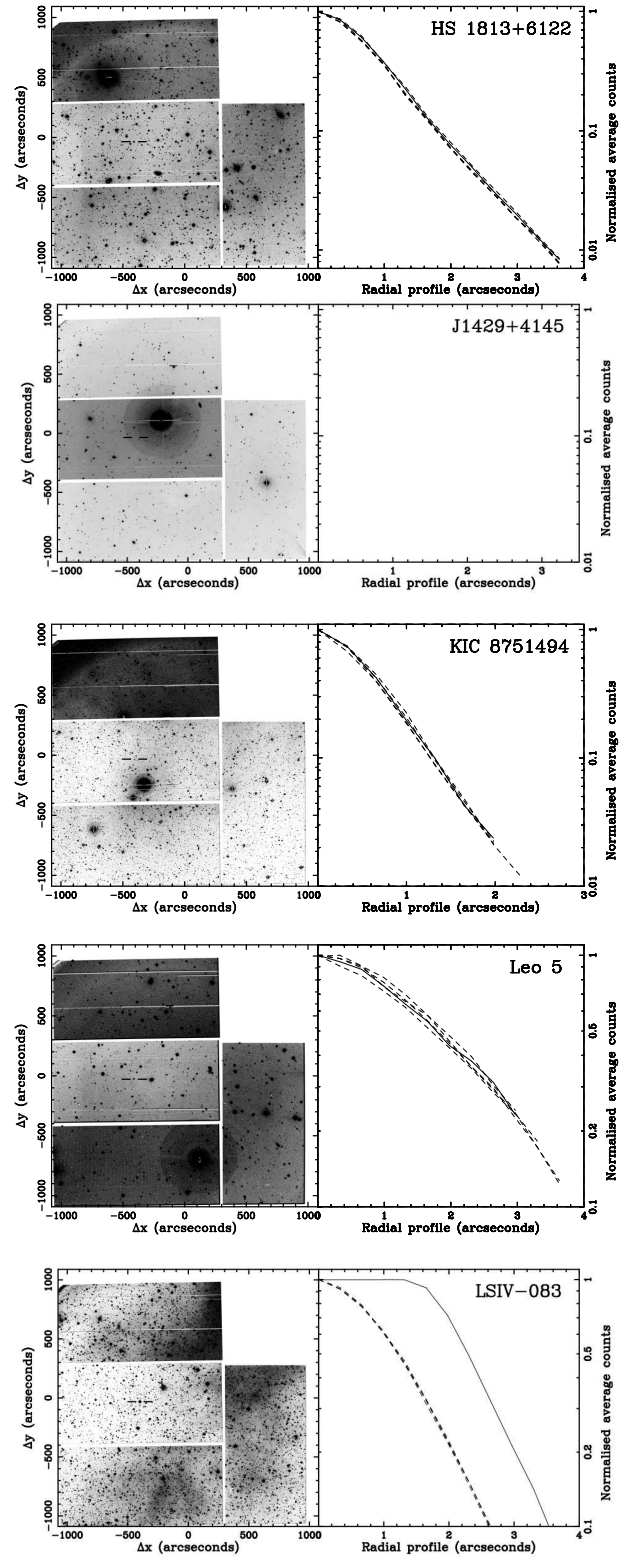
Figure A7. See caption to Figure A1 for details.

Figure A8. See caption to Figure A1 for details.
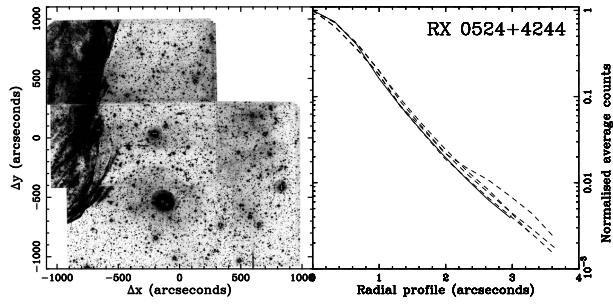

Figure A9. See caption to Figure A1 for details.

Figure A10. See caption to Figure A1 for details.